Hybrid Bladder Phantom to Validate Next-Generation Optical Wearables for Neurogenic Bladder Volume Monitoring

Kelsey J. Tu[1], Jesse H. Lam[2], Byeong-Il Kang[2], Aram Kim[3,4,*], Sehwan Kim[1,4,*]

[1]Department of Biomedical Engineering, School of Medicine, Dankook University, Cheonan, Korea
[2]Beckman Laser Institute Korea, School of Medicine, Dankook University, Cheonan, Korea
[3]Department of Urology and Neurogenic Bladder Clinic, Konkuk University Medical Center, Konkuk University School of Medicine, Seoul, Korea
[4]Medithings Co., Ltd., Seoul, Korea

Purpose: The development of optics-based wearables for bladder volume monitoring has emerged as a significant topic in recent years. Given the innovative nature of this technology, there is currently no bladder phantom available to effectively validate these devices against more established gold standards, such as ultrasound. In this study, we showcase and demonstrate the performance of our hybrid bladder phantom by using an optical device and making comparisons with ultrasound.
Methods: A series of validation tests, including phantom repeatability, ultrasound scanning, and an optical test, were performed. A near-infrared optical device was utilized to conduct diffuse optical spectroscopy (DOS). Machine learning models were employed to construct predictive models of volume using optical signals.
Results: The size and position of an embedded balloon, serving as an analog for the bladder, were shown to be consistent when infused with 100 mL to 350 mL of water during repeatability testing. For DOS data, we present 7 types of machine learning-based models based on different optical signals. The 2 best-performing models demonstrated an average absolute volume error ranging from 12.7 mL to 19.0 mL.
Conclusions: In this study, we introduced a hybrid bladder phantom designed for the validation of near-infrared spectroscopy-based bladder monitoring devices in comparison with ultrasound techniques. By offering a reproducible and robust validation tool, we aim to support the advancement of next-generation optical wearables for bladder volume monitoring.

Keywords: Bladder volume phantom; Near-infrared spectroscopy validation; Neurogenic bladder; Ultrasound

INTRODUCTION

Neurogenic bladder (NB) is a dysfunction of the nervous pathway that leads to a loss of voluntary bladder control [1]. NB may manifest as a symptom of various medical conditions, including spinal cord injury (SCI), multiple sclerosis, and stroke. It is estimated that in the United States, 80% of individuals with SCI, 40%–90% of those with multiple sclerosis, and 15% of stroke

Corresponding author: Aram Kim https://orcid.org/0000-0002-2055-2262
Department of Urology, Konkuk University Medical Center, Konkuk University School of Medicine, 120-2 Neungdong-ro, Gwangjin-gu, Seoul 05030, Korea
Email: arkim@kuh.ac.kr
Co-corresponding author: Sehwan Kim https://orcid.org/0000-0002-5491-3732
Department of Biomedical Engineering, School of Medicine, Dankook University, 119 Dandae-ro, Dongnam-gu, Cheonan 31116, Korea
Email: paul.kim@dankook.ac.kr
Submitted: October 16, 2023 / **Accepted after revision:** November 15, 2023

survivors will experience some degree of NB [2]. One of the most significant challenges affecting the quality of life for those with NB is their inability to perceive bladder fullness [3]. Common issues for patients with NB include bladder overfilling, urinary tract infections (UTIs), bladder stones, kidney failure, and involuntary leakage during sleep or in social situations.

Ultrasound devices are typically bulky and cumbersome, and their operation requires trained medical personnel. Furthermore, they are economically infeasible for personal use, often costing thousands of United States dollars [4, 5]. To address this issue, proposals have been made for the development of a compact, lightweight, and wearable device capable of measuring bladder volume in real time [6-8].

Near-infrared spectroscopy (NIRS) is an emerging technology for monitoring bladder fullness. NIRS is a noninvasive optical technique that operates in the near-infrared wavelength range (approximately 650–1,000 nm) [9]. This range is particularly well-suited for deep tissue interrogation, such as bladder monitoring, because tissue absorption is relatively low, allowing the light to penetrate deeper and interact with subsurface structures. Using NIRS, biomarkers like tissue optical properties and chromophore concentrations can be determined [10, 11]. As a wearable device, NIRS devices can be made extremely compact with the use of modern light-emitting diodes and detectors. Additionally, NIRS does not require a coupling medium, which makes it more convenient for patients than ultrasonic techniques that necessitate regular application of sonographic gel. These advantages have been recognized by several groups, who have proposed NIRS for bladder-related applications [12, 13].

In this paper, we showcase the development and validation of a bladder-simulating phantom constructed from silicone and synthetic gelatin (SG) materials. We employed machine learning techniques to create models that predict volume based on optical data obtained from diffuse optical spectroscopy (DOS) [14, 15]. Our goal was to establish a reliable validation platform for the forthcoming generation of light-based bladder volume monitoring devices.

MATERIALS AND METHODS

To create a phantom that is compatible with both NIRS and ultrasound, several materials were evaluated. Silicone is a popular choice for NIRS phantoms because of its optical flexibility and its refractive index, which closely matches that of human tissue [16]. However, silicone has poor acoustic properties, making it unsuitable for deep ultrasound scanning [17]. Organic gelatin and agar have been utilized for both optical and ultrasound purposes [18, 19], but they degrade quickly and possess mechanical properties that can render them exceedingly delicate. SG, a newer option for optical uses, boasts a prolonged shelf life and proven ultrasound compatibility [20]. Nevertheless, the high viscosity of SG in its liquid form, its hydrophobic nature, and its swift curing time posed challenges in incorporating standard optical absorbers and scatterers like nigrosin and titanium dioxide. Thus, we engineered a hybrid phantom to meet the demands of both imaging technologies.

As depicted in Fig. 1, the hybrid bladder phantom was constructed with one sidewall made of optically customized sili-
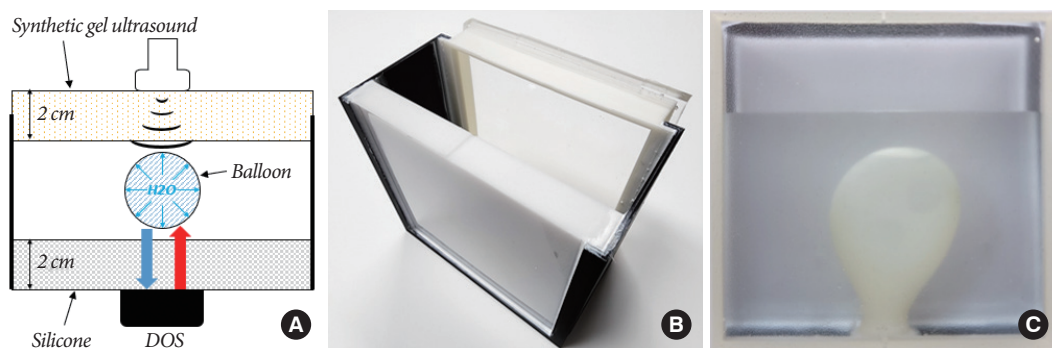
Fig. 1. A bladder phantom compatible with optical and ultrasonic technology. (A) Diagram of the bladder phantom operation, with direct optical spectroscopy (DOS) on the silicone side and ultrasound on the synthetic gelatin (SG) side. Both the silicone and SG layers were 2 cm in thickness. The balloon is in the center and expands to fill the lumen of the enclosure. (B) A diagonal view of the constructed phantom showcasing the turbid silicone and transparent SG walls. (C) Viewing through the SG wall to observe the partially inflated balloon. The phantom was filled with water in this photo for demonstration purposes, but is typically filled with a scattering fluid.

cone, and the opposite wall was fashioned from SG material suitable for ultrasonic applications. These walls were affixed to a 3-dimensional (3D)-printed box. At the phantom's center, a latex balloon served as the bladder analog, secured to a port. A silicone tube was threaded into the balloon, with an attached syringe enabling the regulation of the water volume within. Both walls had a uniform thickness of 2 cm and were arranged to ensure that their distances to the balloon were roughly equivalent.

Fabrication of the Silicone Wall

To fabricate the silicone wall, we followed a procedure similar to that described by Cerussi et al. [16]. Briefly, 0.585 g of titanium IV dioxide (TiO_2, 248576, Sigma Aldrich, St. Louis, MO, USA) was weighed out into an empty beaker. Into the same beaker, we added 60 mL of P4 silicone activator (Eager Plastics, Chicago, IL, USA), then placed it in a sonicator (Branson 3800; Sigma Aldrich) for 3 hours. During sonication, we added 1 mL of 1.5 g/L nigrosin ink (198285, Sigma Aldrich) and 2 mL of 1.5 g/L NIR979W dye (QCR Solutions, Port St. Lucie, FL, USA) to 600 mL of P4 silicone base (Eager Plastics). We blended the contents with a handheld mixer until fully homogenized. The silicone activator with TiO_2 was then slowly introduced into the silicone base with stirring until completely homogenized. The mixture was placed inside a vacuum chamber to de-aerate before being transferred to a silicone mold. The filled mold was placed back into the vacuum chamber until no bubbles remained. Finally, the silicone was allowed to cure for 24 hours.

Fabrication of the SG Wall

For the construction of the SG wall, 700 g of clear gelatin (Humimic Medical, Greenville, SC, USA) was cut into approximately 3-cm cubes and placed inside a 1,000 mL beaker. A mechanical oven (Heratherm OS630, Thomas Scientific, Swedesboro, NJ, USA) was preheated to 125°C. The beaker containing the gelatin was then placed in the oven until the SG was completely melted, which took approximately 3 hours. After melting, the SG was poured into a deep aluminum pan. Subsequently, a custom 3D-printed frame constructed from acrylonitrile butadiene styrene (ABS) was immersed in the pan to ensure that the thickness of the SG, once set, would match that of the silicone wall. The frame was then left in the pan to cure overnight.

Final Assembly of the Phantom

After curing both the silicone and SG walls, the phantom assembly commenced. The silicone wall was positioned, and sili-

cone glue was meticulously applied to all junctions between the silicone and the box. Likewise, sealant was applied to the SG frame. A 3D-printed ring was inserted into the neck of the balloon to secure the tubing. Subsequently, the balloon was positioned over the box's bottom hole and sealed. The completed phantom's overall dimensions were 16×17×11.5 cm.

Preparation of the Filling Medium

A 70% fat-to-water content emulsion was prepared as the filling medium, following a procedure similar to that described by Ohmae et al. [18]. In a 1,000 mL beaker, 965 g of food-grade pure soybean oil was mixed with 15 g of lecithin emulsifier (Daejung Chemicals & Metals Co., Ltd., Siheung, Korea) and heated on a hotplate to 60°C until the lecithin had completely dissolved. Concurrently, 420 g of water was heated to the same temperature in another 1,000-mL beaker. The 2 liquids were then combined using a high-speed vacuum blender (i8800, Jiaxiang Electric Co., Ltd., Dongguan, China), employing a preset blending routine that lasted for a total of 2 minutes and 30 seconds. After blending, the emulsion was allowed to cool for 5 minutes before being poured into the phantom.

Balloon Reproducibility

The reproducibility of the phantom, specifically the ability to inflate the balloon consistently in the same position and manner using the syringe's labeled guidance, was evaluated using imaging techniques. In this experiment, the phantom was filled with clear water, and the balloon was incrementally inflated from 50 mL to 350 mL, which is the syringe's maximum capacity, in 50 mL increments. At each increment, the balloon was imaged by looking through the transparent SG wall. This procedure was then replicated twice. Additionally, careful attention was given to maintaining the camera and phantom in identical positions for each imaging step. Variations in the balloon's size and position were assessed by calculating the percentage difference on a pixel-by-pixel basis.

Optical Device and the Application of Machine Learning

DOS, a quantitative optical modality that operates in the near-infrared spectrum, was utilized to measure our phantom [21-24]. In brief, DOS is capable of estimating the optical properties of turbid media, specifically absorption (μ_a) and reduced scattering (μ_s'). It fundamentally integrates 2 techniques: the frequency domain (FD), which relies on laser light captured by a photodetector, and the continuous wave (CW), which uses white light

detected by a spectrometer. The construction and description of a DOS-based device have been extensively detailed in previous studies [14, 15].

For our experiment, a probe was 3D-printed with a source-to-detector distance of 30 mm. This probe was subsequently mounted to ensure consistent positioning on the silicone side of the hybrid SG phantom for the duration of the experiment.

To estimate bladder volume using optical signals data collected from a DOS-based device were analyzed with machine learning models employing multiple linear regression (MLR). MLR is a supervised learning method that uses multiple independent variables to predict a single dependent variable [25]. Seven MLR models were used, each based on different types of optical signals gathered by the FD and CW components. These signals varied from basic detector outputs, such as amplitude, phase, and reflectance, to more processed signals, namely absorption coefficient (μ_a) and reduced scattering coefficient (μ_s'). The models were trained on data from a single inflation set ranging from 100 mL to 300 mL, in increments of 100 mL. We predicted bladder volume using each MLR model as the phantom bladder was repeatedly filled and emptied, with volumes ranging from 100 mL to 350 mL in 50 mL increments. Data analysis was conducted using MATLAB 2020b.

Validation With Ultrasound

In this study, we used a commercial ultrasound device (Bio-con-1100, Mcube Technology Co., Ltd., Seoul, Korea) as the gold-standard reference. We validated the expected volume of the balloon with ultrasound measurements ranging from 100 mL to 350 mL, increasing in 50-mL increments. This validation served 2 purposes: (1) to confirm that our phantom could provide adequate contrast for ultrasound imaging, and (2) to ensure the accuracy of the volume delivered by the syringe. In accordance with the manufacturer's recommendations, we performed 3 ultrasound measurements at each increment and selected the maximum volume from these 3 measurements for use.

RESULTS

Bladder Phantom Volume Reproducibility

Based on photographic analysis, as depicted in Fig. 2, we noted variations in the balloon's position and shape when inflated to only 50 mL. The minimal internal pressure at this volume led to a partial collapse and wrinkling of the balloon's surface, which varied with each inflation. However, when the balloon was further inflated to 100 mL and then to a maximum of 350 mL, we observed a more consistent reproducibility in terms of the balloon's position, shape, and size. Consequently, for subsequent experiments involving ultrasound and DOS, we omitted the 50 mL inflation step and employed only volumes exceeding 100 mL.

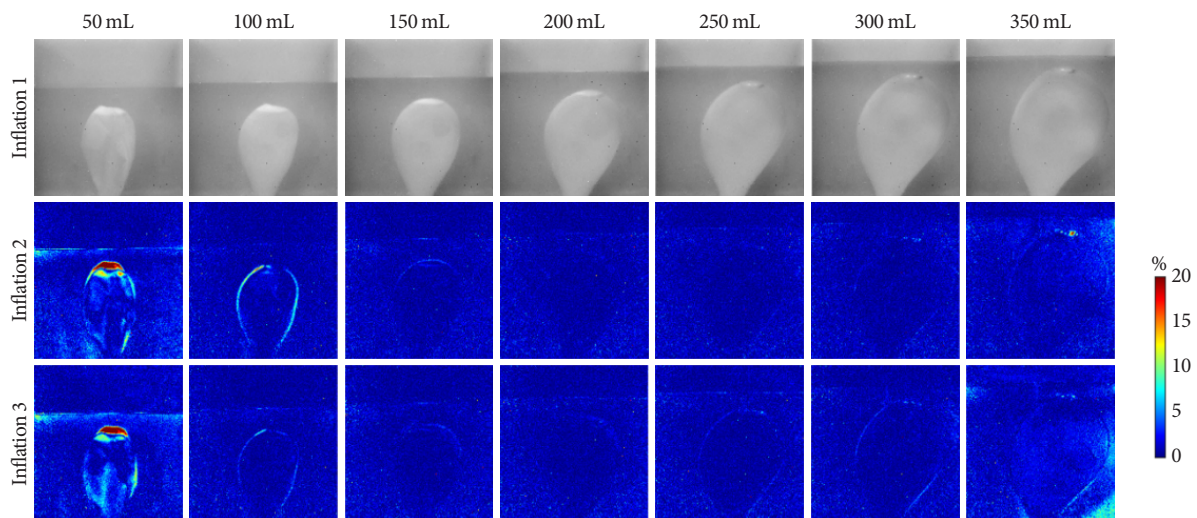**Fig. 2.** The reproducibility of our bladder phantom was tested by repeatedly photographing at specific volume intervals. The pixel intensity percent differences are shown in the middle and bottom rows, revealing changes in balloon position and shape as it was reinflated. Blue indicates small changes, while red indicates larger changes. The first inflation cycle was used as a baseline for the subsequent cycles.

DOS Combined With Machine Learning Results

Different types of data captured by the DOS were categorized into separate MLR models. The R^2 and mean absolute volume error for each model were calculated to evaluate their perfor-

Table 1. Data obtained through DOS using the FD and CW methods, as well as estimated optical properties

Model No.	Data	R^2	Mean absolute error (mL)
1	Amplitude (FD)	0.977[a]	19.0
2	Phase (FD)	0.060	78.2
3	μ_a (FD)	0.763	47.0
4	μ_s' (FD)	0.890	23.8
5	Reflectance (CW)	0.928[a]	15.4
6	μ_a (CW)	0.969[a]	12.7
7	μ_s' (CW)	0.942[a]	17.7

Various multiple linear regression volume prediction models can be generated depending on the type of data utilized. The coefficient of determination for each model and mean absolute error compared to the expected balloon volume are shown.
DOS, diffuse optical spectroscopy; FD, frequency domain; CW, continuous wave.
[a]Models with an $R^2 > 0.900$ are shown as the best-performing models.

mance, as presented in Table 1. If R^2 is deemed the most critical parameter, then model 1 and model 6 would be regarded as the top-performing models. Conversely, if one prioritizes the lowest mean absolute error, model 5 and model 6 emerge as the best. Predictions of bladder volume based on the MLR models with the highest R^2 are illustrated in Fig. 3. The trends are remarkably consistent, especially as the balloon volume was cycled between 100 mL and 350 mL. The most significant error occurred at the final volume increment to 350 mL.

Validation With Ultrasound

The expected balloon volume, as indicated by the syringe labeling, was validated through ultrasound imaging. We found an average absolute volume difference of 8.3 mL when compared to the anticipated volume, as depicted in Fig. 4. This degree of absolute volume error aligns with the manufacturer's data [26].

DISCUSSION

While ultrasound has long been the clinical standard for noninvasive bladder volume measurements, it still presents many limitations for personal use in wearable devices. Recent research suggests that NIRS-based wearables for bladder volume monitoring could be a promising new direction [27]. However, dur-
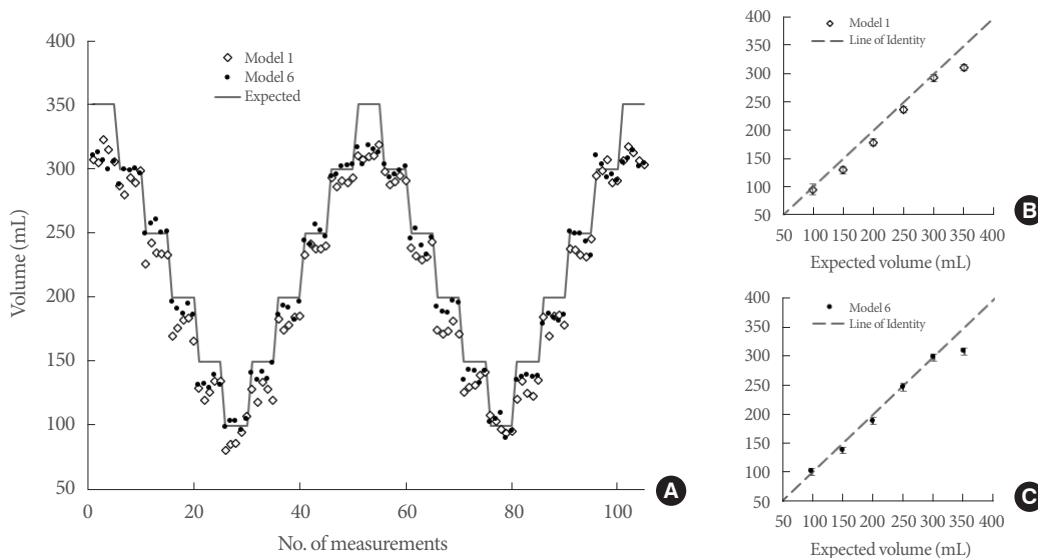

Fig. 3. The 2 best-performing models (as selected by the highest R^2 values) are presented here. (A) The balloon volume was repeatedly cycled between the maximum and minimum volume and tracked by the diffuse optical spectroscopy device. Five optical measurements were performed at each volume step. The expected (syringe) volume and the volume estimated by the 2 models are also shown. (B) For model 1, unique volume steps were averaged with the standard deviation shown in red and compared against the expected volumes. (C) Likewise, the mean and standard deviation for each volume step are shown for model 6.

ing the development of such devices, it is crucial to compare NIRS with ultrasound-based technologies. To facilitate this comparison, a reliable bladder phantom that can accommodate
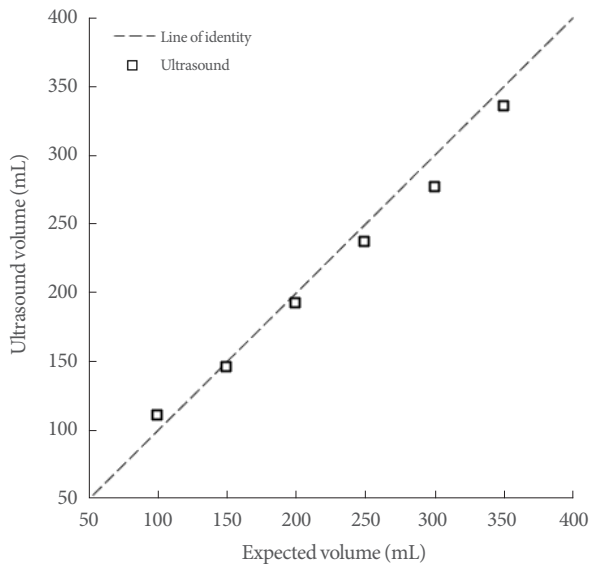

Fig. 4. A commercial bladder volume ultrasound device was used to calculate the volume of the balloon in our phantom. This helped validate the construction of the phantom, which was designed to mimic the human bladder, as well as the accuracy of our expected volume (syringe volume). The mean absolute error was found to be 8.3 mL, which was within the manufacturer's stated error.

both technologies is important. In this work, we surveyed various materials suitable for bladder phantoms and have created a phantom using SG and silicone. We demonstrate how this phantom can serve as a robust validation platform, simplifying the evaluation of devices and comparison of techniques in this field.

This research has significant clinical implications. Currently, ultrasound is the internationally accepted method to measure bladder urine volume. However, ultrasound devices are cumbersome, costly, and intended for operation by medical professionals. For accurate measurement, patients must stay still and lie in a supine position as a healthcare provider manipulates the ultrasound equipment over the lower abdomen to assess bladder urine volume.

For NB patients, residual urine volume is a critical concern. However, the frequent use of medical facilities for bladder monitoring via ultrasound is impractical. This raises critical questions: When is the optimal time for self-catheterization? Should it be performed on a fixed schedule, or in response to any perceived need to urinate? Postponing self-catheterization can lead to complications such as bladder overdistension, recurrent UTIs, incontinence, and even kidney damage. Conversely, excessive self-catheterization may increase the risk of urethral injury and UTIs, while also negatively impacting quality of life by restricting regular work and social activities.

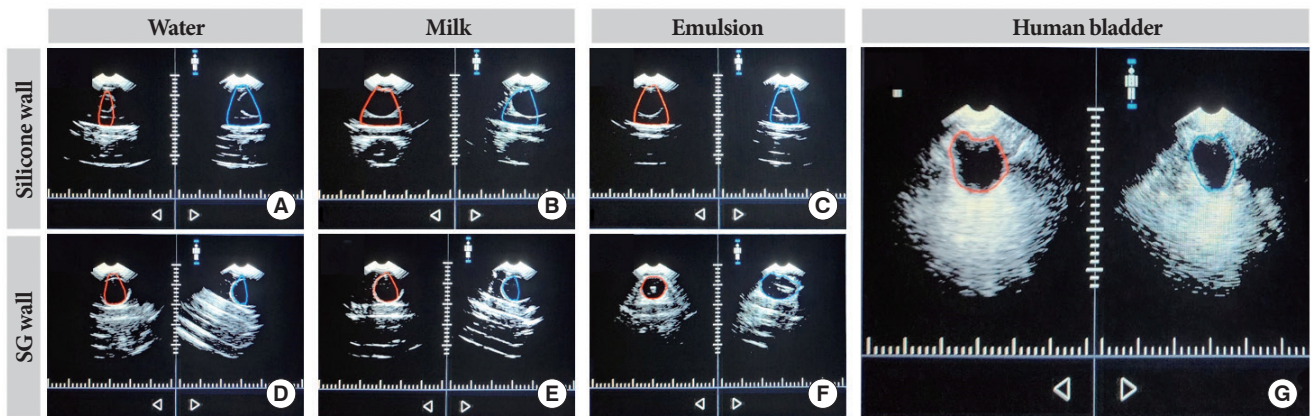These concerns are also applicable to elderly patients with

Fig. 5. Ultrasound results comparing silicone and synthetic gelatin (SG) walls using water, 2% milk, or emulsion as filling medium and a human bladder reference with an expected volume of approximately 250 mL for all images. In addition, the red and blue outlines in all images represent the bladder posterior (red) and anterior (blue) generated by ultrasound. (A–C) Shows inaccurate detection of the posterior and anterior locations of the balloon when using 2% milk or water through the silicone wall. (D, E) With water or 2% milk through the SG wall, inaccurate detection of the posterior and anterior locations can be seen. (F) The emulsion medium results are shown, with the posterior and anterior locations being properly detected through the SG wall. (G) An ultrasound reference image of a human bladder.

conditions such as Alzheimer disease. Often, we encounter elderly patients in the clinic with excessively full bladders after they have undergone computed tomography or abdominal ultrasound examinations. Unfortunately, for these patients, there are often no alternative solutions except for the use of an indwelling urinary catheter. However, wearable devices that enable a caretaker to monitor bladder urine volume in real time could represent a paradigm shift, alleviating many of these issues. One potential technology that could be used for this application is NIRS.

To facilitate the development of NIRS-based bladder volume monitors, we aimed to create an appropriate validation phantom. Silicone has traditionally been a preferred material for NIRS technologies due to its optical versatility [16]. However, its acoustic properties were deemed unsatisfactory [17]. In Fig. 5A–C, we observed significant attenuation of ultrasonic waves, which resulted in minimal contrast. In contrast, SG material demonstrated better compatibility with ultrasonic waves, as shown in Fig. 5D–F. Nonetheless, we discovered that the choice of filling medium greatly influenced image contrast. Utilizing a high lipid emulsion as the medium (Fig. 5E) allowed our ultrasound device to accurately determine the balloon volume while remaining compatible with NIRS. Consequently, we adopted a hybrid approach to construct the phantom, using silicone for the optical components and SG for the ultrasonic elements.

For the assembly of the phantom, it was desirable to achieve a strong, watertight seal between the silicone and the SG walls. Although silicone sealant typically adheres well to the material of the silicone phantom, we noted a weak bond when applied to SG. This required the introduction of an intermediary layer. To address this, we 3D-printed a frame to secure the SG, and the silicone glue was then applied to the frame. For the 3D printing of this frame, we recommend using ABS rather than polylactic acid because ABS has a higher melting point, making it less prone to warping when in contact with SG that has been melted at 125°C.

Thus, our experience in fabricating these phantoms can be distilled into the following points: (1) A silicone wall serves as an optically customizable medium for NIRS applications. (2) An optically turbid filling liquid is required to ensure adequate scattering. (3) SG is compatible with ultrasound imaging; however, the composition of the filling liquid must differ from that of the balloon's to provide the necessary contrast. (4) Standard silicone glue does not adhere well to SG, necessitating the use of an ABS frame for phantom construction.

Designing a repeatable phantom was essential. During repeatability testing with volumes of 100 mL and above, the balloon's size and position proved to be highly consistent. However, at 50 mL, we suspect that the balloon's surface lacked sufficient tension to prevent collapse, leading to uncontrollable creases and folds. The size and position of the balloon were also inconsistent at volumes below 100 mL. Nevertheless, in scenarios requiring a balloon at low or near-zero volumes, one potential solution could be to apply constant tension to the balloon, such as by attaching a string or magnet to its top.

Further analysis of DOS data can be used to guide the design of compact NIRS devices. The DOS instrument used in this study is not a wearable device; its size and weight are comparable to that of a consumer microwave. However, the wealth of data provided by DOS allows the identification of which optical signals are most sensitive to changes in volume. Consequently, a more compact version could be developed that includes only the most critical technologies, rather than the entire suite of components found in DOS.

Using the different types of data from the DOS instrument produced volume predictive models with varying degrees of fit and accuracy. In this work, we utilized MLR. Although a range of more sophisticated machine learning models could be employed for data analysis [28], such exploration was outside the purview of our current research. Nevertheless, our MLR models performed remarkably well, with some nearly matching the accuracy of ultrasound measurements and exhibiting a high R^2 value.

This work has several limitations. Although the results of these experiments are promising, they do not fully replicate the complexity and variability of the human body. For instance, factors such as the presence of hemoglobin, bones, and anatomical differences between biological genders were not accounted for. More sophisticated phantoms could be developed by including these elements. Of course, there is no substitute for in vivo testing. Therefore, we recommend using this phantom as a consistent platform to validate, assess, and compare the theoretical performance of NIRS devices. Another limitation is the use of a 2 cm silicone wall to simulate the human abdomen. In a healthy individual, the adipose layer thickness of the abdomen can range from 1.5 cm to 2.1 cm [29]. However, in obese individuals, the thickness of the abdominal wall can exceed 4 cm [30].

In this study, we presented a hybrid phantom compatible with both NIRS and ultrasonic technologies. We detailed the construction steps, demonstrated the phantom's consistency,

and validated the inflation volume using ultrasonic methods. Additionally, by employing DOS, we showcased the utility of this phantom and applied machine learning to construct MLR models for predicting optical volume based on FD and CW modalities. We then assessed the various models, with several achieving accuracy levels comparable to those of ultrasound. We anticipate that our work will aid in the advancement of next-generation NIRS-based bladder monitoring devices, ultimately enhancing the quality of life for NB patients.

AUTHOR CONTRIBUTION STATEMENT

· Conceptualization: *KJT, JHL, BIK, AK, SK*
· Data curation: *KJT, JHL*
· Formal analysis: *KJT, JHL, BIK, AK, SK*
· Funding acquisition: *BIK, AK, SK*
· Methodology: *KJT, JHL, BIK, AK, SK*
· Project administration: *BIK, AK, SK*
· Visualization: *KJT, JHL, BIK*
· Writing - original draft: *KJT, JHL, BIK, AK*
· Writing - review & editing: *KJT, JHL, BIK, AK, SK*

ORCID

Kelsey J. Tu	0009-0008-6200-4716
Jesse H. Lam	0000-0002-2113-779X
Byeong-Il Kang	0009-0009-3219-507X
Aram Kim	0000-0002-2055-2262
Sehwan Kim	0000-0002-5491-3732

REFERENCES

1. Manack A, Motsko SP, Haag-Molkenteller C, Dmochowski RR, Goehring EL, Nguyen-Khoa BA, et al. Epidemiology and health-care utilization of neurogenic bladder patients in a us claims database: epidemiology of neurogenic bladder. Neurourol Urodyn 2011; 30:395-401.

2. Dorsher PT, McIntosh PM. Neurogenic bladder. Adv Urol 2012; 2012:816274.

3. Wheeler TL, De Groat W, Eisner K, Emmanuel A, French J, Grill W, et al. Translating promising strategies for bowel and bladder management in spinal cord injury. Exp Neurol 2018;306:169-76.

4. Byun SS, Kim HH, Lee E, Paick JS, Kamg W, Oh SJ. Accuracy of bladder volume determinations by ultrasonography: are they accurate over entire bladder volume range? Urology 2003;62:656-60.

5. Yip SK, Sahota D, Chang AMZ. Determining the reliability of ultrasound measurements and the validity of the formulae for ultrasound estimation of postvoid residual bladder volume in postpartum women. Neurourol Urodyn 2003;22:255-60.

6. Fechner P, König F, Kratsch W, Lockl J, Röglinger M. Near-infrared spectroscopy for bladder monitoring: a machine learning approach. ACM Trans Manage Inf Syst 2023;14:1-23.

7. Kang BI, Kim A, Kim S. Advancing patient care: innovative use of near-infrared spectroscopy for monitoring urine volume in neurogenic bladder. Int Neurourol J 2023;27(Suppl 1):S27-33.

8. Van Leuteren PG, Klijn AJ, de Jong TPVM, Dik P. SENS-U: validation of a wearable ultrasonic bladder monitor in children during urodynamic studies. J Pediatr Urol 2018;14:569.e1-569.e6.

9. Ferrari M, Mottola L, Quaresima V. Principles, techniques, and limitations of near infrared spectroscopy. Can J Appl Physiol 2004; 29:463-87.

10. Shah N, Cerussi A, Eker C, Espinoza J, Butler J, Fishkin J, et al. Noninvasive functional optical spectroscopy of human breast tissue. Proc Natl Acad Sci USA 2001;98:4420-5.

11. Ohmae E, Yoshizawa N, Yoshimoto K, Hayashi M, Wada H, Mimura T, et al. Comparison of lipid and water contents by time-domain diffuse optical spectroscopy and dual-energy computed tomography in breast cancer patients. Appl Sci 2019;9:1482.

12. Molavi B, Shadgan B, Macnab AJ, Dumont GA. Noninvasive optical monitoring of bladder filling to capacity using a wireless near infrared spectroscopy device. IEEE Trans Biomed Circuits Syst 2014;8:325-33.

13. Fong DD, Yu X, Mao J, Saffarpour M, Gupta P, Abueshsheikh R, et al. Restoring the sense of bladder fullness for spinal cord injury patients. Smart Health 2018;9-10:12-22.

14. Pham TH, Coquoz O, Fishkin JB, Anderson E, Tromberg BJ. Broad bandwidth frequency domain instrument for quantitative tissue optical spectroscopy. Rev Sci Instrum 2000;71:2500-13.

15. Bevilacqua F, Berger AJ, Cerussi AE, Jakubowski D, Tromberg BJ. Broadband absorption spectroscopy in turbid media by combined frequency-domain and steady-state methods. Appl Opt 2000;39: 6498-507.

16. Cerussi AE, Warren R, Hill B, Roblyer D, Leproux A, Durkin AF, et al. Tissue phantoms in multicenter clinical trials for diffuse optical technologies. Biomed Opt Express 2012;3:966-71.

17. Zell K, Sperl JI, Vogel MW, Niessner R, Haisch C. Acoustical properties of selected tissue phantom materials for ultrasound imaging. Phys Med Biol 2007;52:N475-84.

18. Ohmae E, Yoshizawa N, Yoshimoto K, Hayashi M, Wada H, Mimura T, et al. Stable tissue-simulating phantoms with various water and

lipid contents for diffuse optical spectroscopy. Biomed Opt Express 2018;9:5792-808.

19. Özdemir M, Özdemir G, Eroğul O. Investigating ballistic gelatin based phantom properties for ultrasound training. In: Lhotska L, Sukupova L, Lacković I, Ibbott GS, editors. World Congress on Medical Physics and Biomedical Engineering 2018 [Internet]. Singapore: Springer Nature Singapore; 2019 [cited 2023 Jul 28]. p. 789-93. (IFMBE Proceedings; vol. 68/1). Available from: https://link.springer.com/10.1007/978-981-10-9035-6_145.

20. Morrow DS, Broder J. Cost-effective, reusable, leak-resistant ultrasound-guided vascular access trainer. J Emerg Med 2015;49:313-7.

21. Cerussi A, Shah N, Hsiang D, Durkin A, Butler J, Tromberg BJ. In vivo absorption, scattering, and physiologic properties of 58 malignant breast tumors determined by broadband diffuse optical spectroscopy. J Biomed Opt 2006;11:044005.

22. Ganesan G, Warren RV, Leproux A, Compton M, Cutler K, Wittkopp S, et al. Diffuse optical spectroscopic imaging of subcutaneous adipose tissue metabolic changes during weight loss. Int J Obes 2016;40:1292-300.

23. Warren RV, Cotter J, Ganesan G, Le L, Agustin JP, Duarte B, et al. Noninvasive optical imaging of resistance training adaptations in human muscle. J Biomed Opt 2017;22:1-9.

24. Lam JH, O'Sullivan TD, Park TS, Choi JH, Warren RV, Chen WP, et al. Non-invasive dual-channel broadband diffuse optical spectroscopy of massive hemorrhage and resuscitative endovascular balloon occlusion of the aorta (REBOA) in swine. Mil Med 2018; 183(suppl_1):150-6.

25. Ambrosius WT, editor. Topics in biostatistics. Totowa (NJ): Humana Press; 2007. p. 528.

26. De smit medical. BioCon bladder scanners: frequently asked questions [Internet]. Cromhall (UK): De smit medical; [cited 2023 Aug 4]. Available from: https://www.desmitmedical.com/products/bladder-scanners/bladder-scanner-faqs.

27. Eun SJ. Dynamics in neurourology. Int Neurourol J 2023;27(Suppl 1):S1-2.

28. Kim ES, Shin DJ, Cho ST, Chung KJ. Artificial intelligence-based speech analysis system for medical support. Int Neurourol J 2023; 27:99-105.

29. Anvery N, Wan HT, Dirr MA, Christensen RE, Weil A, Raja S, et al. Utility of high-resolution ultrasound in measuring subcutaneous fat thickness. Lasers Surg Med 2022;54:1189-97.

30. Rolfe EDL, Sleigh A, Finucane FM, Brage S, Stolk RP, Cooper C, et al. Ultrasound measurements of visceral and subcutaneous abdominal thickness to predict abdominal adiposity among older men and women. Obesity 2010;18:625-31.